Cholesteric liquid crystal–carbon nanotube composites with photo-settable reversible and memory electro-optic modes

Oleg Yaroshchuk,[1,*] Sergiy Tomylko,[1] Igor Gvozdovskyy,[1] and Rumiko Yamaguchi[2]

[1]Institute of Physics, NAS of Ukraine, prospect Nauky, 46, Kyiv 03680, Ukraine

[2]EEE Department, Akita University, 1-1 Tegatagakuen-cho, Akita 010-8502, Japan

*Corresponding author: o.yaroshchuk@gmail.com

Received 20 February 2013; revised 30 April 2013; accepted 7 May 2013;
posted 7 May 2013 (Doc. ID 185689); published 7 June 2013

The photoresponsive electro-optical composites based on cholesteric liquid crystal (CLC) with optically controlled chirality and a minute amount of carbon nanotubes (CNTs) are studied. In cells with homeotropic anchoring, these composites exhibit a transition from fingerprint texture to homeotropic nematic texture in the course of photoinduced unwinding of the cholesteric helix. Compared with the CLC counterpart, this transition is much delayed, because of the stabilization of cholesteric filamentary domains by CNTs. The CLC-CNT composites demonstrate dual-mode operation with optical switching between reversible and memory mode. It is found that the memory response is associated with the elastic network of filamentary cholesteric domains that stabilizes the planar CLC texture reached in an electric field. In turn, the reversible mode corresponds to the unwound cholesteric state. Potential applications of this effect are discussed.

OCIS codes: (160.1190) Anisotropic optical materials; (160.2900) Optical storage materials; (160.2100) Electro-optical materials; (160.5335) Photosensitive materials; (310.6845) Thin film devices and applications.

http://dx.doi.org/10.1364/AO.52.000E53

1. Introduction

Liquid crystals (LCs) filled with nanoparticles (NPs) represent a striking example of hybrid composites, which have caused enduring interest over the last decade. This is due to several reasons. First of all, the NPs of inorganic materials can expand the range of properties of LCs, which is determined by their organic nature. LC suspensions of magnetic [1], ferroelectric [2], metal [3], semiconducting [4], and dielectric [5,6] NPs have been developed and extensively studied. Small amounts of these particles substantially modify viscoelastic, dielectric, optical, and electro- and magneto-optical properties of LCs. The other reason is that NPs eliminate inherent undesirable effects in LC layers such as backflow and associated optical bounce, image sticking, optical flicker, etc. [7,8].

One more reason is that the introduction of NPs often leads to new effects not typical for pure LCs. One of them is the effect of electro-optic memory. The essence of this effect is that the LC-NP composite memorizes the state of LC orientation achieved in the electric field. Originally, this effect was discovered for the LC dispersions of pyrogenic silica Aerosil (A) [5,9], where vertical alignment of nematic LC with positive dielectric anisotropy $\Delta\varepsilon$ was stabilized. Based on optical switching from the memorized transparent state to the initial scattering state, a unique optically addressable LCD was proposed [5].

A similar memory effect was recently discovered by our group for LCs doped with carbon nanotubes (CNTs) [10–12]. The difference from the LC-A

1559-128X/13/220E53-07$15.00/0

composites was in the fact that a much smaller (about 100 times less) concentration of NPs was required to achieve a memory state. Another difference was that the memory effect was observed for the LC with $\Delta\varepsilon < 0$. The initial orientation of the LC was homeotropic, while the planar orientation was induced in the electric field and it was partially memorized when the field was off. Stabilizing of the planar alignment comes from the partial alignment of the CNT network in the LC host and the effective LC-CNT interaction. The network acts as a spatially distributed alignment surface and counteracts the elastic torque caused by anchoring with the aligning substrates.

Since the LC-CNT samples switch between two oriented states, they demonstrate essential changes in optical transmittance when viewed between crossed polarizers. This suggests a new principle for information display and storage in the LC-based systems, which can be implemented in memory cells, bistable displays, etc. These applications require essential improvements of the operational parameters of the memory-type LC-CNT composites: first of all, the efficiency, erasure, and recording times of the memory state.

It was demonstrated earlier that the memory efficiency can be doubled and brought close to its maximal value by introducing the optimized amount of chiral dopant (ChD) in the LC host [13]. The induced chirality causes additional force, stabilizing the state of planar orientation realized in an electric field. In developing this idea, in the present study we replace the nonphotosensitive ChD with a photosensitive one. By this way, the system obtains an additional controlling parameter. This can be successfully used to optimize a twisting force for maximal memory and optically switching the samples between different electro-optic modes.

2. Samples and Characterization Methods

As the LC host we used the nematic liquid crystalline mixture MLC6608 from Merck, with a clearing temperature $T_c = 90°C$ and dielectric anisotropy $\Delta\varepsilon = -4.2$. To induce a cholesteric structure, the LC was doped with 2-(4'-phenylbenzylidene)-*p*-menthane-3-one (PBM). This photosensitive left-handed ChD was synthesized at the Institute for Single Crystals, National Academy of Sciences of Ukraine. According to [14], PBM molecules undergo irreversible *trans-cis* isomerization under UV irradiation, and the helical twisting power of *cis* isomers is much lower than that of *trans* isomers. This means that twisting tension in the induced cholesteric LC (CLC) weakens with the irradiation and the material gradually approaches the untwisted state. The concentration of PBM in LC was fixed at 1.4 wt. %. The obtained CLC was mixed by tip sonication with multiwalled CNTs from Spetsmash, Ukraine, having an outer diameter of 20–40 nm and a length of 5–10 μm. The concentration of CNT was 0.02 wt. %. At this value the memory is practically absent, because the network of CNTs is not strong enough to withstand the elastic force caused by homeotropic anchoring [10–12]. As reference samples, pure CLCs were also studied.

The cells were made of glass substrates containing patterned indium-tin oxide (ITO) electrodes. The substrates were spin coated with the layers of homeotropic-type polyimide SE1211 (Nissan, Japan), baked (180°C, 40 min), and unidirectionally rubbed. The cells were assembled so that the rubbing directions of the opposite aligning layers were antiparallel. A cell gap d was maintained by spacers. We commonly used spacers of 16 μm, although the cell thickness was varied in the range of 5–50 μm to determine its effect on the studied properties. The cells were filled with the LC-CNT composites using a capillary method. UV irradiation of the cells was carried out by a high-pressure UV lamp UV-P 280 (Panacol, Germany). The integrated intensity of the light was 6 mW/cm^2.

The LC textures were observed by using a polarizing microscope Polam 213M from LOMO (Russia) equipped with a digital camera conjugated with personal computer. Additionally, the samples were viewed by the naked eye by placing them between a pair of crossed polarizers. The optical transmission T versus applied voltage U curves were measured by the in-house-made electro-optic set up [15]. In these experiments the cell was placed between a pair of crossed polarizers by setting an angle of 45° between the rubbing direction of the cell and the polarization directions of the polarizers. The transmittance of this "sample-polarizer" set was measured as a function of the applied AC voltage ($f = 2$ kHz) by increasing of the voltage stepwise from 0 to 25 V and subsequently decreasing it stepwise to 0. Based on these curves, the memory efficiency was estimated according to the formula

$$M = \frac{T_m - T_0}{T_{\max} - T_0}, \tag{1}$$

where $T_{\max}$, T_0, and T_m are the transmittance values corresponding to maximum of $T(U)$ curve and the initial and final zero-field states, respectively.

3. Results and Discussion

Despite the fact that the photoinduced structural transition "fingerprint texture–homeotropic texture" in the CLC used was earlier studied in [16,17], we return to this issue in order to compare the peculiarities of the structural changes in the samples with nanotubes and those without them at the same exposure conditions. A CLC cell with the areas subjected to different exposure doses is presented in Fig. 1. Intensive scattering before irradiation and for the short exposure dose is caused by the texture of randomly aligned filamentary cholesteric domains (fingers). Formation of the fingers implies that the helical axis is parallel to the plane of the LC cell. At some exposure dose, this texture sharply changes to an unwound (quasinematic) homeotropic texture having a dark appearance when viewed between two crossed

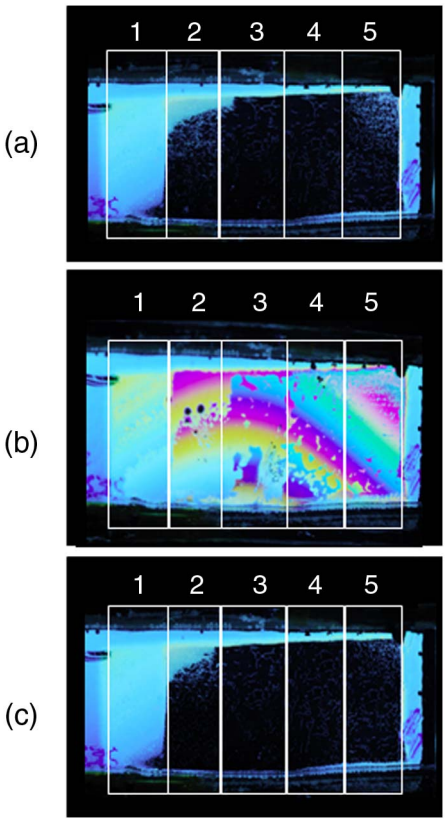

Fig. 1. Photographs of LC cell ($d = 16$ μm) with homeotropic anchoring filled with the cholesteric mixture MLC6608/PBM (1.4 wt. %): (a) before the electric field application, (b) under the field of 25 V, (c) after the field is off. The cell is irradiated with UV light through a proximity mask so that the exposure time is 1, 3, 5, 8, and 20 min in areas 1, 2, 3, 4, and 5, respectively. The cell is viewed between two crossed polarizers.

polarizers. The discontinuous character of this transition was predicted theoretically; the transition comes when the weakening twisting force can no longer overcome the elastic torque determined by the orientational elasticity and anchoring at the boundary substrates. This means that the homeotropic unwound state is achieved before the twisting tension in LC completely vanishes. The limit value of helical pitch $p = p_{\text{th}}$ derived in the approximation of the infinite anchoring energy is [18]

$$p_{\text{th}} = 2d\frac{K_{22}}{K_{33}}, \tag{2}$$

where K_{22} and K_{33} are elastic constants for the twist and bend deformations, respectively, and d is a cell gap.

The exposed areas with the fingerprint texture show insufficient changes under the electric field. At the same time, areas with the homeotropic texture react to the field similarly to nematic LC; because of negative dielectric anisotropy, the LC director reorients perpendicularly to the field (toward the plane of the cell) and returns back to a homeotropic state after the field is off. The difference with the nematic cells is that the CLC cells relax considerably more slowly, seemingly because the twisting force counteracts the elastic torque caused by anchoring at the boundary layers [13].

Figure 2 shows the CLC-CNT cell with exposure domains the same as in the CLC cell (Fig. 1). The corresponding microscope pictures are given in Fig. 3. First, what can be noticed by comparing with pure CLC is a slowing down of the kinetics of structural transformation under the UV light. The exposure range corresponding to the fingerprint texture is

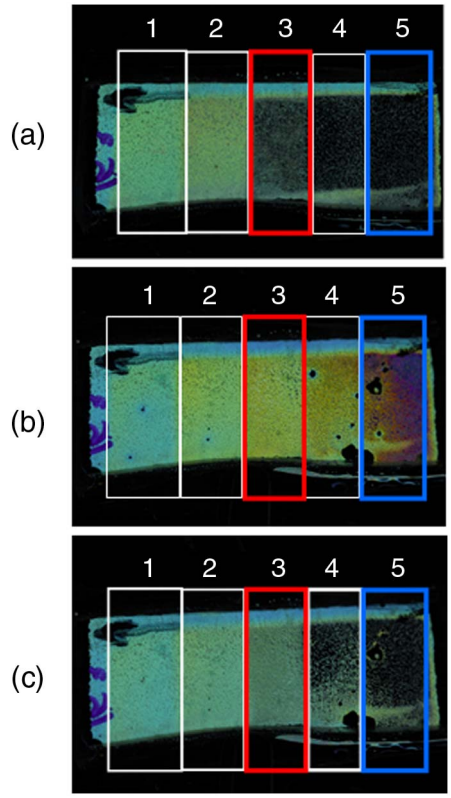

Fig. 2. Photographs of LC cell ($d = 16$ μm) with homeotropic anchoring filled with the composite MLC6608/PBM (1.4 wt. %)–CNT (0.02 wt. %): (a) before the electric field application, (b) under the field of 25 V, (c) after the field is off. The cell is irradiated with UV light through a proximity mask so that the exposure time is 1, 3, 5, 8, and 20 min in areas 1, 2, 3, 4, and 5, respectively. The cell is viewed between two crossed polarizers. The red and blue rectangles mark the exposure domains demonstrating irreversible (memory) and reversible electro-optic response, respectively.

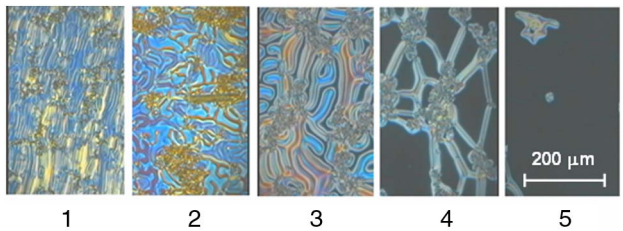

Fig. 3. Microphotographs corresponding to different exposure areas in Fig. 2. Photographs 1, 2, 3, 4, and 5 correspond to the exposure times 1, 3, 5, 8, and 20 min, respectively. The photographs are obtained before application of electric field.

considerably broader. In the initial phase of irradiation, the fingerprint texture is continuous. At higher doses, cholesteric inclusions survive in the homeotropic texture (Fig. 3). These filamentary formations, frequently called oily streaks, form a well-developed network. Due to this network, the structural transition "fingerprint texture–homeotropic nematic texture" becomes diffuse.

These conclusions can be additionally illustrated by photoinduced changes in the period of fingerprint texture Λ, which in case of the continuous texture is proportional to the cholesteric pitch p ($p = 2\Lambda$[19]). The Λ versus exposure time τ_{exp} curves for the CLC and CLC-CNT samples are presented in Fig. 4. Clearly, the cholesteric helix unwinds much faster in pure CLC. Also, the limit value of p defined by Eq. (2) is much lower than that achieved for the CLC-CNT sample. These facts testify to the deceleration of the unwinding of the cholesteric helix under irradiation and its stabilization in the presence of NPs.

The slower structural dynamic in the samples containing CNTs can be partially caused by light absorption with the nanotubes. However, since the concentration of CNTs is incredibly low, this factor hardly plays an important role in our case. The more important reason is believed to be a stabilizing role of CNTs for linear domains of CLC. This is especially clearly seen for the oily streak structures. In CLC, the network of these domains quickly disappears because of interior tension. Usually the domain lines disconnect from the nodes of the network and shrink. The situation in the sample with nanotubes is different. In this case, many domains cling to nanotubes and do not shrink. The domains disconnected from the particles quickly disappear and, as result, the aggregates of CNTs become the nodes of the network of domains. As a consequence, the network becomes

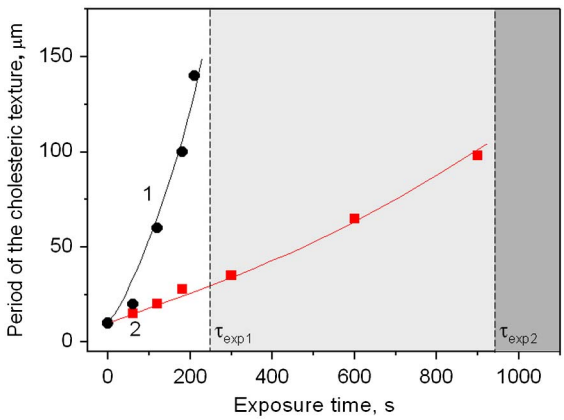

Fig. 4. Period of fingerprint texture as a function of exposure time for CLC (curve 1) and CLC-CNT composite (curve 2) in the cells with $d = 16$ μm. Symbols $\tau_{\text{exp}\,1}$ and $\tau_{\text{exp}\,2}$ denote the exposure times corresponding to "fingerprint–homeotropic quasinematic" textural transition in the CLC and CLC-CNT samples, respectively. For the CLC-CNT series, the range $\tau_{\text{exp}}<\tau_{\text{exp}\,1}$ roughly corresponds to the continuous fingerprint texture and the range $\tau_{\text{exp}\,1}<\tau_{\text{exp}}<\tau_{\text{exp}\,2}$ to the texture of stable oily streaks in homeotropically aligned unwound CLC.

quite stable. It does not disappear completely even after rather long exposure (5 times longer than the one that causes fingerprint–homeotropic transition in pure CLC). It is amazing that the cholesteric domains remain stable even after a strong decrease in the concentration of the ChD, that is, after loss of the twisting force inducing a helical structure.

Zapotocky *et al.* [20] first noted the important role of NPs in the stabilization of a network of linear defects in CLC. These authors showed that due to a colloidally stabilized network of defects, CLCs show unusual properties; similar to nematic colloids [21], they behave as a gel with a solid-like elasticity. The results above demonstrate that in our system the network density, and hence its rigidity, can be controlled by light. In this sense, our composite can be considered as a photoresponsive gel with optically controlled elasticity.

Another advantage of the studied composites is that they show few types of electro-optic response. As is evident from Fig. 1, pure CLC undergoes reversible changes under the electric field in all domains with a homeotropic texture. At the same time, the electro-optical response of the CLC-CNT sample strongly depends on the exposure dose. The short-time irradiated areas 1 and 2 in Fig. 2 barely respond to the field. In area 3 favorable conditions for the memory effect are met. Initially this area shows almost perfect homeotropic alignment with only slight scattering, caused by the oily streak network. After the field application cycle, the homeotropic alignment was changed to the random planar alignment that macroscopically manifests itself in residual brightening, which is registered both visually and in electro-optic tests (Fig. 5a). The induced memory state was erasable by several factors: heating the sample above T_c, additional UV irradiation, and mechanical stress. A further increase of the exposure dose resulted in an even better dark state (area 5), meaning that the network of defects was eliminated. This exposed area demonstrates reversible electro-optical response (Fig. 5b).

To explain the difference in the electro-optic response of areas 3 and 5 in Fig. 2, we consider changes in their microscopic structure under the applied field. According to Fig. 6, pure CLC restores its initial texture after the field application cycle. At the same time, the sample doped with CNTs partially retains the planar orientation induced in an electric field. It can be seen that the remaining islands of planar orientation fill the meshes of the network of oily streaks and thus are stabilized by this network. Note the difference from the previously described mechanism of memory for a nematic LC [10–12]. In that system, the network of nanotubes was a major factor in stabilizing the planar orientation of the LC. In case of CLC the role of the nanotubes basically comes down to stabilizing the network of linear cholesteric domains, which in turn supports the planar orientation of the CLC after switching off the electric field. We do not consider here the issue of essential

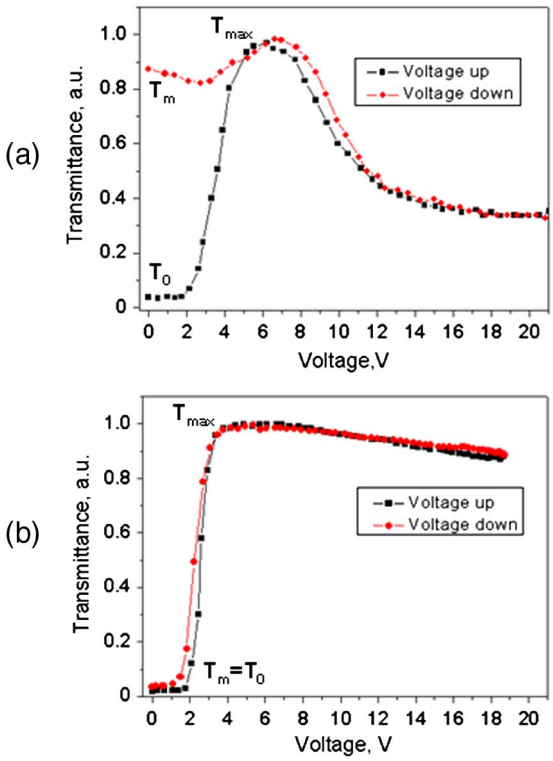

Fig. 5. Transmittance versus voltage curves corresponding to exposure areas (a) 3, and (b) 5, in Fig. 2.

concentrations of nanotubes. One can predict a key role of CNT networks in the memorization of planar orientation in the case of a totally unwound cholesteric state, were oily streak formations of the cholesteric phase are absent.

The described regularities remain in the range of thicknesses of CLC-CNT layers $d = 5$–25 μm. Generally, the lower the thickness d, the faster the photoinduced transition from fingerprint texture to homeotropic nematic texture. At $d > 25$ μm, this structural transition became blurry even in pure CLC, due to increased stability of oily streaks. At $d \leq 5$ μm there was the problem of blocking of the CNTs

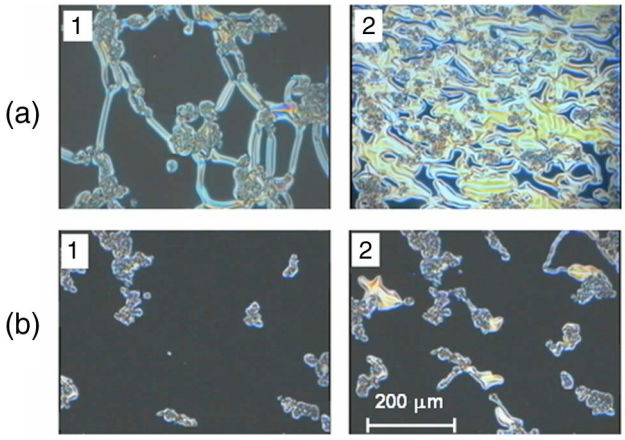

Fig. 6. Microphotographs corresponding to exposure areas (a) 3, and (b) 5, in Fig. 2. In each row, photo 1 shows the domain texture before the voltage application and photo 2 the texture of the same area after the voltage is off.

at the entrance to the cell when filling the composites by the capillary method.

Since the role of CNTs in our system is reduced to stabilizing the network of cholesteric defects, it can be assumed that the nanotubes can be replaced with any other particles. However, we believe that using the nanotubes (i.e., strongly elongated particles) minimizes concentration of NPs needed to stabilize the network of linear cholesteric domains. As mentioned above, the use of elongated CNTs instead of spherical NPs of A in memory-type composites reduced the particle concentration by about 100 times [11,12]. Furthermore, the nanotubes can impart quite interesting dielectric properties to the CLC, as is the case for nematic LCs [22].

Finally, we consider the practical aspects of these results. The continuous decrease in the concentration of a ChD with UV irradiation can be used to replace the time-consuming preoptimization of ChD [13] by simple *in situ* optimization. By setting a proper exposure dose, the sample can be adjusted for the memory or reversible electro-optic mode. It is important that the memory effect in the studied composites can be reached at a smaller concentration of nanotubes compared with the composites based on nematic LCs. This considerably reduces the probability of electric breakdown. The memory efficiency

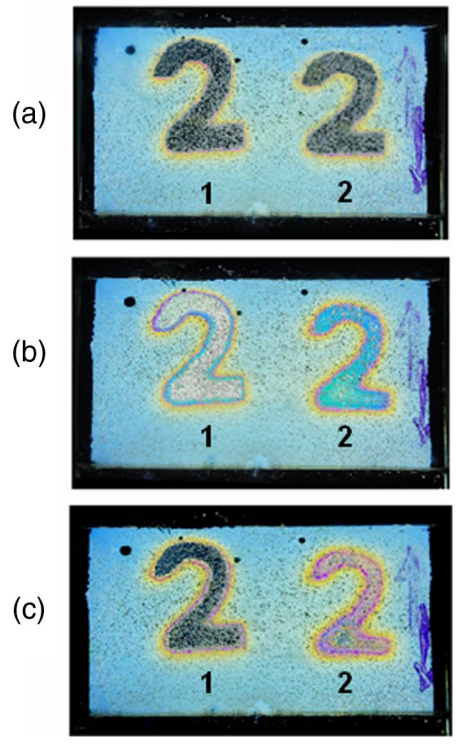

Fig. 7. Principle of an optically switchable dual-mode LCD. The cell filled with the MLC 6608/PBM (1.4 wt. %)–CNT (0.02 wt. %) composite is exposed through the "2" shaped window to UV light for 15 and 5 min in areas 1 and 2, respectively. Photographs a–c correspond to the initial state, field-on state, and field-off state of the cell, respectively, viewed between a pair of crossed polarizers. It is evident that area 1 operates in reversible mode and area 2 in memory mode.

attained in the best samples was $M = 0.8–0.9$, i.e., similar to and even higher than that earlier achieved for the CLC-CNT samples based on the optically insensitive ChD [13], approaching its maximum possible value. Thus, keeping the merits of previously studied composites, optically settable composites have more room for optimization and control.

The results above suggest a new principle for a dual-mode LCD with an optically settable memory and reversible electro-optic modes. These two modes can be realized simultaneously in different parts of the same LCD by using electric addressing of image formation. On the other hand, one can suggest a unique display principle with optical addressing and electro-optic activation. For optical recording, one can utilize masking as illustrated in Fig. 7 or beam scanning principle [5]. The recorded image appears after activation of the composite layer with an electric field. The same idea can be used to design elements of optical memory with optical addressing and electro-optical activation. The UV light in all these devices can be used not only for presetting but also for erasing the memory state.

The downside of the CLC used is irreversible photoconversion of the ChD's molecules. Future use of ChDs with two optically switchable isomers of different chiralities will allow us to implement reversible optical switching between the mentioned electro-optic modes. Such dopants have been recently developed and successfully used for controlling planar CLC textures [23,24].

4. Conclusions

This paper studied the effect of a minute amount of CNTs on the structural transitions and electro-optic response of photosensitive CLC, earlier investigated in [15,16]. In cells with homeotropic anchoring, this material demonstrates photostimulated structural transitions from a fingerprint to a homeotropic texture with oily streak inclusions, and eventually to a pure homeotropic texture. This occurs due to a gradual decrease of twisting tension in the cells in the course of the photoconversion of the ChD. Compared with the case of pure CLC, the samples doped with CNTs show slower dynamic of structural changes and a stable network of oily streaks in the homeotropic structure of unwound CLC. The latter texture yields an irreversible (memory) electro-optic response, because the network of cholesteric domains stabilizes the planar orientation of CLC achieved in an electric field. In turn, the pure homeotropic texture demonstrates a reversible electro-optic response.

In situ optimization of ChD concentration for the memory and reversible responses is quite attractive for applications. It suggests a new principle for dual-mode LCDs, which are currently actively discussed [25–27]. This principle allows both photo and electrical addressing of image formation. In addition, it can be the basis for the elements of optical memory with optical addressing and electro-optic activation. Use of minute amounts of CNTs minimizes the risk of electric breakdown in the cells as well as distortion of the cholesteric structure.

O. Yaroshchuk acknowledges the Japan Society for Promotion of Science Award L-10535.

References

1. S.-H. Chen and N. M. Amer, "Observation of macroscopic collective behavior and new texture in magnetically doped liquid crystals," Phys. Rev. Lett. **51**, 2298–2301 (1983).
2. F. Li, O. Buchnev, C. I. Cheon, A. Glushchenko, V. Reshetnyak, Y. Reznikov, T. Sluckin, and J. West, "Orientational coupling amplification in ferroelectric nematic colloids," Phys. Rev. Lett. **97**, 147801 (2006).
3. Y. Shiraishi, N. Toshima, K. Maeda, H. Yoshikawa, J. Xu, and S. Kobayashi, "Frequency modulation response of liquid crystal electro-optic device doped with nanoparticles," Appl. Phys. Lett. **81**, 2845–2847 (2002).
4. T. Zhang, C. Zhong, and J. Xu, "CdS-nanoparticle-doped liquid crystal displays showing low threshold voltage," Jpn. J. Appl. Phys. **48**, 055002 (2009).
5. M. Kreuzer, T. Tschudi, and R. Eidenschink, "Erasable optical storage in bistable liquid crystal cells," Mol. Cryst. Liq. Cryst. Sci. Technol., Sect. A **223**, 219–227 (1992).
6. M. Boxtel, R. Janssen, C. Bastiaansen, and D. Broer, "Visco-elastic liquid crystal colloids for the continuous processing of twisted nematic electro-optical cells," J. Appl. Phys. **89**, 838–842 (2001).
7. H. Qi and T. Hegmann, "Impact of nanoscale particles and carbon nanotubes on current and future generations of liquid crystal displays," J. Mater. Chem. **18**, 3288–3294 (2008).
8. M. Rahman and W. Lee, "Scientific duo of carbon nanotubes and nematic liquid crystals," J. Phys. D **42**, 063001 (2009).
9. A. Glushchenko, H. Kresse, V. Reshetnyak, Y. Reznikov, and O. Yaroshchuk, "Memory effect in filled nematic liquid crystals," Liq. Cryst. **23**, 241–246 (1997).
10. L. Dolgov, O. Yaroshchuk, and N. Lebovka, "Effect of electro-optic memory in liquid crystals doped with carbon nanotubes," Mol. Cryst. Liq. Cryst. **496**, 212–229 (2008).
11. L. Dolgov, N. Lebovka, and O. Yaroshchuk, "Effect of electro-optic memory in suspensions of carbon nanotubes in liquid crystal," Colloid J. **71**, 603–611 (2009).
12. L. Dolgov, O. Yaroshchuk, S. Tomylko, and N. Lebovka, "Electro-optical memory of a nematic liquid crystal doped by multi-walled carbon nanotubes," Condens. Matter Phys. **15**, 33401 (2012).
13. L. Dolgov, S. Tomylko, T. Semikina, O. Koval'chuk, and O. Yaroshchuk, "Carbon nanotube doped liquid crystals: robust composites with a function of electro-optic memory," Diam. Relat. Mater. **19**, 567–572 (2010).
14. S. N. Yarmolenko, L. A. Kutulya, V. V. Vaschenko, and L. V. Chepeleva, "Photosensitive chiral dopants with high twisting power," Liq. Cryst. **16**, 877–882 (1994).
15. A. Kovalchuk, S. Zakrevska, O. Yaroshchuk, and U. Maschke, "Electrooptical properties of three-component compositions liquid crystal-aerosil-photopolymer," Mol. Cryst. Liq. Cryst. **368**, 129–136 (2001).
16. Yu. Reznikov and T. Sergan, "Orientational transitions in a cell with twisted nematic liquid crystal," Mol. Cryst. Liq. Cryst. **330**, 375–381 (1999).
17. I. Gvozdovskyy, O. Yaroshchuk, M. Serbina, and R. Yamaguchi, "Photoinduced helical inversion in cholesteric liquid crystal cells with homeotropic anchoring," Opt. Express **20**, 3499–3508 (2012).
18. B. Y. Zeldovich and N. V. Tabiryan, "Equilibrium structure of a cholesteric with homeotropic orientation on the walls," Sov. Phys. JETP **56**, 563–566 (1982).
19. V. G. Chigrinov, V. V. Belyaev, S. V. Belyaev, and M. F. Grebenkin, "Instabilities of cholesteric liquid crystals in an electric field," Sov. Phys. JETP **50**, 994–999 (1979).
20. M. Zapotocky, L. Ramos, P. Poulin, T. C. Lubensky, and D. A. Weitz, "Particle-stabilized defect gel in cholesteric liquid crystals," Science **283**, 209–212 (1999).

21. T. A. Wood, J. S. Lintuvuori, A. B. Schofield, D. Marenduzzo, and W. C. K. Poon, "A self-quenched defect glass in a colloid-nematic liquid crystal composite," Science **334**, 79–83 (2011).
22. L. Dolgov, S. Tomylko, O. Koval'chuk, N. Lebovka, and O. Yaroshchuk, "Liquid crystal dispersions of carbon nanotubes: dielectric, electro-optical and structural peculiarities," in *Carbon Nanotubes*, J. M. Marulanda, ed. (Intech, 2010), Chap. 24, pp. 451–484, http://sciyo.com/books/show/title/carbon-nanotubes.
23. J. Ma, Ya. Li, T. White, A. Urbas, and Q. Li, "Light-driven nanoscale chiral molecular switch: reversible dynamic full range color phototuning," Chem. Commun. **46**, 3463–3465 (2010).
24. M. Mathews, R. S. Zola, S. Hurley, D. K. Yang, T. J. White, T. J. Bunning, and Q. Li, "Light-driven reversible handedness inversion in self-organized helical superstructures," J. Am. Chem. Soc. **132**, 18361–18366 (2010).
25. C.-Y. Huang, C.-C. Lai, Y.-H. Tseng, Y.-T. Yang, C.-J. Tien, and K.-Y. Lo, "Silica-nanoparticle-doped nematic display with multistable and dynamic modes," Appl. Phys. Lett. **92**, 221908 (2008).
26. C.-Y. Huang, C.-C. Lai, Y.-J. Huang, and J.-H. Chen, "Switching characteristics of silica nanoparticle-doped dual-mode liquid crystal device," Jpn. J. Appl. Phys. **49**, 028003 (2010).
27. J.-H. Lee, D.-H. Song, T. Kim, H.-K. Shin, C.-G. Jhun, S.-B. Kwon, D.-G. Kim, W. S. Kim, T.-H. Yoon, and J. C. Kim, "Reflective dual mode liquid crystal display with dynamic mode utilizing the transition behavior between the two stable states of its memory mode," Jpn. J. Appl. Phys. **50**, 084101 (2011).